Chapter 4
Harvesting Signal Power from Constructive Interference in Multiuser Downlinks

Christos Masouros

4.1 Introduction to Constructive Interference: Definitions, Examples, and Classification

Interference is traditionally considered as the major limitation in meeting the ever-increasing demands for transmission rates and quality of service (QoS) in current and future wireless communication systems. In multi-user and multi-access communications, interference is typically manifested in the communication channel, where signals of different links are superimposed. Particular effort has been placed on utilizing the channel's state information (CSI) to counteract its effects on transmission. It has been shown that in both time- and frequency-division duplex modes the CSI can be made known to the transmitter (a situation termed as CSIT). The a priori knowledge of interference is therefore not an uncommon situation and it is in fact readily available at the cellular base stations during downlink transmission, when CSIT combined with the knowledge of all data symbols intended for transmission can be used to predict the resulting interference between the symbols.

The seminal work of Costa in [1] has shown by information-theoretic analysis that in the cases where CSIT is available, known interference does not affect the capacity of the broadcast channel, which is therefore equivalent to the respective noise-only channel. In [1] it is also stressed that the optimum strategy to achieve this capacity would be to invest power not in cancelling interference, but rather in coding along interference. Nevertheless, the majority of existing transmission strategies attempt to eliminate, cancel, or pre-subtract interference. Indeed, a number of important technologies exist that make use of the channel knowledge to mitigate

C. Masouros (✉)
University College London, Torrington Place, London, UK
e-mail: chris.masouros@ieee.org

D.N.K. Jayakody et al. (eds.), *Wireless Information and Power Transfer: A New Paradigm for Green Communications*, DOI 10.1007/978-3-319-56669-6_4

or manage interference. Only recently, however, there has been a rising interest in making use of the interference power to enhance the useful signal [2, 3].

What justifies the traditional interference-cancellation approaches is that, from a statistical perspective, interference imposes a "random," noise-like perturbation to the transmitted information and introduces a variance to the received signal which on average hinders detection and deteriorates the resulting performance. By employing an instantaneous, as opposed to statistical, view of interference one can see that interference can contribute to the detection of the useful signal and in fact, act as a source of useful signal power. This phenomenon can be utilized in the CSIT-assisted downlink transmission and other known-interference scenarios where interference can be predicted, and its power can be harvested to improve the wireless link's performance. In modern systems where transmitted power is becoming a scarce resource and energy efficiency is becoming more and more central in the overall network design, the harvesting and use of signal power from interference which is inherent in the communication system provides an important source of green useful power for reliable signal detection.

4.1.1 Is All Interference Harmful? Examples and Definitions

To motivate the concept of interference exploitation, this section presents a qualitative analysis of instantaneous interference and explores the possibility of treating part of interference as constructive, as a step towards the design of innovative transmission schemes.

A trivial example of a two-user link is shown in Fig. 4.1a, where we define the desired symbol of user 1 as u_1 and the interfering symbol from user 2 as u_2. For simplicity, and without loss of generality, let us assume that these belong to a Binary Phase Shift Keying (BPSK) constellation and that $u_1 = 1, u_2 = -1$. For illustration purposes, ignore the noise at the receiver, and assume a lossless channel from the

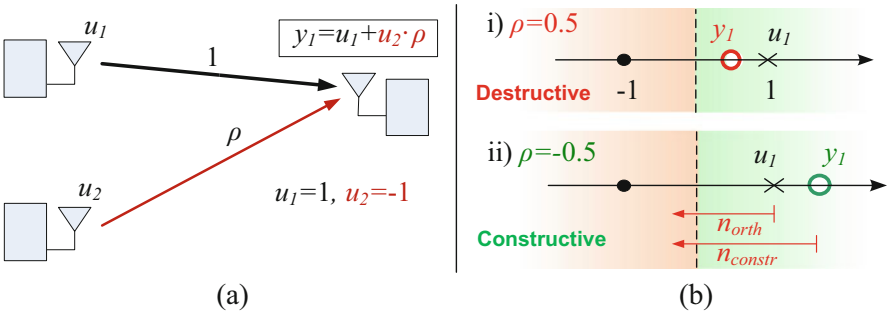

Fig. 4.1 The concept of constructive interference—a two-user example: (**a**) transmission scenario, (**b**) destructive (*i*) and constructive (*ii*) interference

intended transmitter to the receiver and an interfering channel represented by the coefficient ρ. Accordingly, the received signal can be expressed as

$$y_1 = u_1 + u_2 \cdot \rho, \tag{4.1}$$

where $u_2 \cdot \rho$ is the interference. Note that this model also corresponds to a multiple-input-single-output (MISO) transmission with a matched filtering receiver tuned to the channel of user 1, where the correlation between the two channels is ρ [4]. In Fig. 4.1b two distinct cases are shown, depicting the transmitted ($\times$) and received (o) symbols for user 1 on the BPSK constellation. In case (i) with $\rho = 0.5$ it can be seen from (4.1) that $y_1 = 0.5$. In this case, the destructive interference from user 2 has caused the received symbol of user 1 to move towards the decision threshold (denoted by the dashed line) in the BPSK constellation. The received power of user 1 has been reduced and its detection is prone to low-power noise. In case (ii), however, for $\rho = -0.5$, the system equation (4.1) yields $y_1 = 1.5$, and hence the interference from user 2 is constructive. The power received by user 1 has been augmented due to the interference from user 2 and now its detection is tolerant to noise n_{constr} of higher power compared to n_{orth} for the orthogonal transmission case without interference. It should be stressed that in both cases the transmit power for each user in this elementary example is equal to one. Note that, while the above example refers to a two-user transmission scenario for illustration purposes, the fundamental concept can be extended to more users, multipath transmission, inter-cell interference in a multi-cell environment, and other generic interference-limited systems.

Let us make the above observation more explicit, by looking at the geometrical representation in a two-user example with arbitrary channels. In Fig. 4.2 we show a scenario of two users with channels h_1 and h_2. One could think of this as a multiple-input-single-output (MISO) channel with two transmit antennas and one receive antenna. To focus the study on the interference between the two transmissions, in line with the above example, noise is also assumed to be zero here. In both subfigures, the axes depict the directions of the complex-valued channels, and $u_1 = 1, u_2 = -1$ like in the case above. The bold-lined arrow in each subfigure represents the received signal y and the purple arrows denote its projection to each

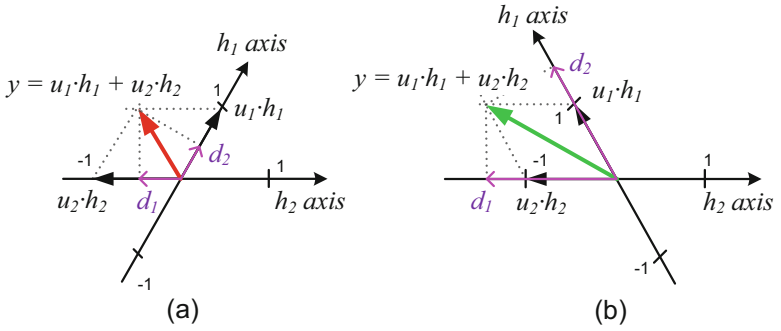

Fig. 4.2 Geometrical representations of interference scenarios: (**a**) destructive, (**b**) constructive

of the channel axes which represents the match-filtered symbols d_1, d_2 at the receiver before the decision stage. In the case of Fig. 4.2a, the two transmitted symbols add up destructively in the received signal y. Consequently, the projections d_1, d_2 of the received signal on the channel axes yield reduced symbol energy compared to the transmitted symbols u_1, u_2 and the detection is destructively affected by interference. In the case of Fig. 4.2b, however, the addition of the users' transmitted symbols yields a received signal which has higher amplitude compared to the destructive case. As a result, the detected symbols d_1, d_2 have higher amplitudes compared to the destructive case, and more importantly compared to the transmitted symbols u_1, u_2 themselves, which in a practical scenario and in the presence of noise translate to higher signal to noise ratios (SNRs).

Note that in both cases the amplitude of the transmitted symbols u_1, u_2 (and hence the transmitted power) is the same, and it is the interfering power that increases the received amplitude (hence the SNR) in the second case. Moreover, note that in the case where different combinations of symbols u_1, u_2 are transmitted, the configurations of Fig. 4.2a, b may result in constructive and destructive interference, respectively. In other words, a channel configuration that yields constructive interference for a specific symbol combination may result in destructive interference for other combinations and vice versa. It is clear from the above that the characterization of interference and its separation into constructive–destructive depends not only on the correlation of the transmission paths but also on the instantaneous symbol values.

4.1.2 Systematic Classification of Interference for Generic Constellations

To utilize the above observations and take advantage of constructive interference in a systematic way in practical scenarios, it is important to be able to classify interference into constructive and destructive systematically. Accordingly, here we discuss the mathematical classification of interference for a number of PSK and QAM constellations.

Let us first derive the mathematical classification criteria for PSK modulation. Figure 4.3a–c shows Monte Carlo generated received constellation points for different PSK modulations. These are represented by randomly positioned dots in the PSK constellations, centered around the nominal PSK constellation points. The red dots denote received signals corrupted by destructive interference while the green dots represent received symbols resulting from constructive interference. The generic criterion for constructive/destructive interference classification is as follows:

Constructive interference is that which yields received signals that have increased distances from the decision boundaries of the modulated-symbol constellation, with respect to the nominal constellation points.

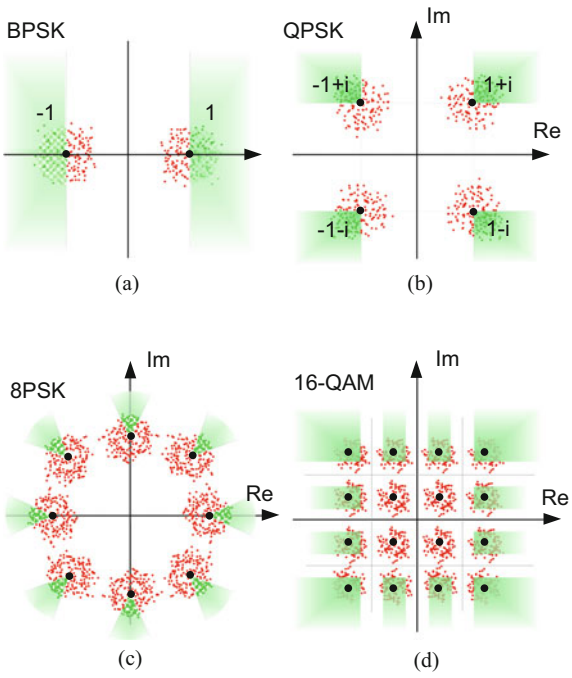

Fig. 4.3 Basic PSK and QAM constellations and constructive (*green*)–destructive (*red*) interference sectors

Note that this is a simplistic definition of constructive interference, where the comparison is made to the nominal constellation points. In the context of SNR optimization, we will see in Sect. 4.2.2 that the definition can be extended to arbitrary distances from the constellation's decision boundaries to reflect varying SNR and QoS requirements for the communication links. Based on the above definition, below we derive the mathematical criteria for constructive interference for BPSK, QPSK, and generic M-PSK modulation.

BPSK Let us take a closer look at Fig. 4.3a, and let us we define $u_i = e^{j\phi_i}$ as the PSK symbol of interest and y_i as the received signal without noise, for the ith user. Accordingly, the interference to the ith user can be found as $g_i = y_i - u_i$. For the BPSK modulation of Fig. 4.3a the desired user's signal $u_i \in \{-1, +1\}$, and therefore the decision boundary is the imaginary axis. Constructive interference pushes the received symbol away from the decision boundary, and therefore for $u_i = -1$ interference is constructive when its real part is negative, and for $u_i = 1$ interference is constructive when it's positive. Accordingly, for BPSK, interference is constructive when

$$\mathrm{Re}(u_i)\mathrm{Re}(g_i) \geq 0 \tag{4.2}$$

QPSK For quadrature-PSK (QPSK) modulation, since there are two decision boundaries (the real and imaginary axes) in the signal constellation, the above

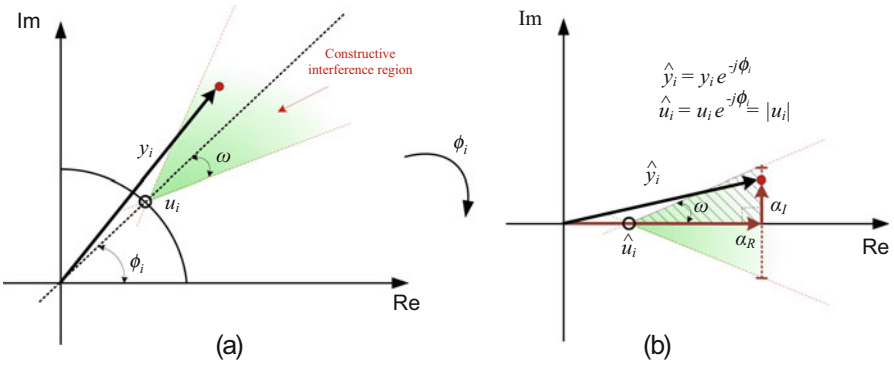

Fig. 4.4 Interference classification for M-PSK constellations

criterion has to be applied separately to the real and imaginary part of the received signal. Therefore, for QPSK, interference is constructive when

$$\mathrm{Re}(u_i)\mathrm{Re}(g_i) \geq 0 \;\&\; \mathrm{Im}(u_i)\mathrm{Im}(g_i) \geq 0 \tag{4.3}$$

Again, the received symbols that satisfy this requirement are shown in green color in Fig. 4.3b.

Interference Classification for *M*-PSK To obtain a more generic characterization of interference for M-PSK, let us observe the constellation example shown in the diagram of Fig. 4.4a, which focuses on one out of the M possible constellation points in the modulated-symbol constellation, namely the point with symbol phase ϕ_i. The constructive interference region denoted by the green shaded area spans an angle on each side of ϕ_i that depends on the order M of the modulation, and is defined by the parameter ω for which

$$\omega = \frac{\pi}{M} \tag{4.4}$$

To obtain a generic characterization irrespective of the specific constellation point studied, let us rotate our observation by $-\phi_i$ as shown in Fig. 4.4b, where

$$\hat{y}_i = y_i e^{-j\phi_i} \tag{4.5}$$

Applying the same transformation to the symbol of interest results in

$$\hat{u}_i = u_i e^{-j\phi_i} = |u_i| \tag{4.6}$$

i.e., we have now isolated the amplitude of the desired symbol. Let us also define $\alpha_R = \mathrm{Re}(\hat{y}_i)$ and $\alpha_I = \mathrm{Im}(\hat{y}_i)$, where clearly, α_R represents the amplitude of

the received constellation point due to constructive interference and α_I provides a measure of the angle shift from the phase of the original constellation point.

For constructive interference conditions to hold, it can be seen that α_R and α_I are allowed to grow infinitely, as long as their ratio is such that the received symbol is contained within the constructive area of the constellation, i.e., the green shaded area in Fig. 4.4b. Using basic geometry in the right triangle denoted by the diagonal stripes in the figure we have that, for the received symbol to fall inside the constructive interference region, α_I, α_R have to obey

$$|\alpha_I| \leq (\alpha_R - |u_i|) \tan \omega \tag{4.7}$$

In other words, for an M-PSK modulation for which the constellation points are normalized to unit power, the resulting interference is constructive when the received symbol (excluding noise) follows

$$\left|\mathrm{Re}(y_i e^{-j\phi_i})\right| \leq (\mathrm{Im}(y_i e^{-j\phi_i}) - 1) \tan \omega \tag{4.8}$$

where ϕ_i is the desired information and ω is the modulation-dependent parameter as defined above.

Analytical characterization criteria of the interference for B-, Q-, and higher order PSK modulation are further detailed in [5, 6]. We shall generalize the above to accommodate arbitrary SNR requirements in the beamforming optimization discussion of Sect. 4.2.2.

Constructive Interference in QAM Constellations It was shown in the previous section that there are benefits to be gained from utilizing interference in PSK-based communication systems. Notably, low order PSK appears in numerous scenarios in many communication standards [7]. Indeed BPSK and QPSK are favored in high interference scenarios where the achievable rates are limited due to the ill-conditioned nature of the channel or the density of the communication access points. Evidently, the more the interference, the more the gain from utilizing it as opposed to eliminating it. In a highly correlated or a densely populated multi-access channel conventional schemes would employ low order PSK modulation and invest most of their power in canceling the existing interference, so it is in these scenarios where it is expected to gain the most from exploiting interference.

For the completeness of the discussion, however, we must not omit situations where higher transmission rates are achievable, in which case higher order QAM would be used according to the communication standards. It is therefore reasonable to raise the following questions: "Can the above concept be applied to QAM constellations?," "How much benefit can be extracted from interference energy in these cases?". A first attempt to address these issues is presented in [8, 9] and more recently in [10–12]. To examine this, let us observe the 16-QAM constellation, shown in Fig. 4.3d. It can be seen that for the inner constellation points, since they are bounded by decision thresholds in all directions around them, the concept of constructive interference does not hold. Interference that shifts the received

inner constellation point away from one decision boundary pushes it closer to another decision boundary. However, for the outer constellation points there is still some space for constructive interference. Indeed for the points at the corners of the 16-QAM constellation the conditions are identical to the ones for the QPSK constellation points. Therefore, as shown in Fig. 4.3d the interference classification criteria for these points are similar to the ones discussed above. Moreover, for the outer constellation points in-between the corner points again there exists a margin of constructive interference as shown in Fig. 4.3d, strictly towards the directions away from the inner decision boundaries, as shown by the green shaded areas. Combining the above observations, we can design the constructive interference criteria for the example of 16-QAM defined by the alphabet $\mathscr{A} = \{\eta^r + i\eta^i | \eta^r, \eta^i \in \{\pm 1, \pm 3\}\}$ as [10]

$$\begin{aligned} \mathrm{Re}(u_i)\mathrm{Re}(g_i) \geq 0 \;\&\; \mathrm{Im}(u_i)\mathrm{Im}(g_i) \geq 0, &\quad \text{for } u_i \in \{\pm 3 \pm i3\} \\ \mathrm{Re}(u_i)\mathrm{Re}(g_i) \geq 0 \;\&\; \mathrm{Im}(g_i) = 0, &\quad \text{for } u_i \in \{\pm 3 \pm i\} \\ \mathrm{Re}(g_i) = 0 \;\&\; \mathrm{Im}(u_i)\mathrm{Im}(g_i) \geq 0, &\quad \text{for } u_i \in \{\pm 1 \pm i3\} \\ \emptyset, &\quad \text{for } u_i \in \{\pm 1 \pm i\} \end{aligned} \tag{4.9}$$

4.1.2.1 Decision-Boundary Adaptation

Notably, from the above discussion it follows that constructive interference does not apply for the inner constellation points of QAM constellations, which increase in population as the order of QAM modulation increases. However, further scope for accommodating constructive interference in QAM constellations can be provided by employing adaptive, channel-dependent, decision boundaries in the receive constellation. This concept is illustrated in Fig. 4.5. Based on a stochastic study of the

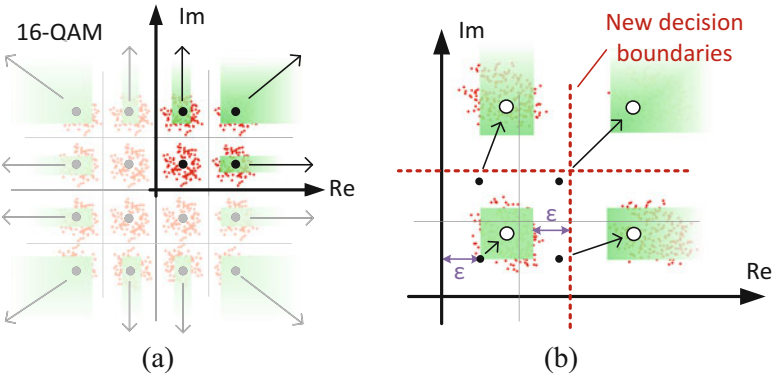

Fig. 4.5 Decision-boundary expansion for 16-QAM: (**a**) 16-QAM with fixed decision boundaries, (**b**) boundary expansion to accommodate constructive interference

power of constructive interference for a given communication scenario, one could envisage an expansion of the decision boundaries of the QAM constellation such that the whole constellation spreads to accommodate an expansion of the Euclidean distances between all constellation points. This would allow for additional constructive interference for all constellation points, including the inner points. The resulting effect is shown in Fig. 4.5b where the focus is on the top right quadrant of the 16-QAM constellation, and the black dots represent the original constellation points, while the circles represent the expanded constellation points. The distances from the constellation points to the decision boundaries in the original constellation are denoted as ε. It can be seen that the new constellation points can move within the green shaded areas, while maintaining an equal or greater minimum Euclidean distance ε from the new decision thresholds compared to the distance in the original constellation. Importantly, this allows for constructive interference power to be accommodated for the inner constellation points, that had no provision for constructive interference when employing fixed decision boundaries as in Fig. 4.5a.

These remarks indicate that, while the advantages of interference exploitation are more pronounced in systems using PSK modulation, there are still benefits to be gained in QAM-based systems. While initial efforts have been made towards this direction in [11], it is yet to be explored how to optimally expand the decision boundaries of QAM to accommodate interference, and how the above qualitative observations quantify in performance gain for the QAM constellations.

Early work carried out on simple precoding techniques that will be discussed in the following indicates that there are significant benefits to be derived by the above observations. The important feature is that these benefits are drawn not by increasing the transmitted power of the useful signals u_i, but rather by the reuse of interference energy that already exists in the communication system; a source of green signal energy that with conventional interference-cancellation techniques is left unexploited.

4.2 Constructive Interference in Multiuser Downlinks: Harvesting Useful Signal Power

To illustrate the usefulness of the above observations, we shall overview a number of techniques that exploit constructive interference superposition, focusing on the baseline scenario of single-cell multiuser downlink transmission. We note, however, that interference-exploitation approaches have also been developed for multi-cell scenarios in cognitive radio applications [13–16].

Accordingly, consider a multiuser MISO (MU-MISO) downlink that consists of a base station transmitter equipped with N_t antennas and K single-antenna receivers. For the case of the closed-form precoders of [5, 6, 8–11, 17–20], it is required that $N_t \geq K$. The above channel is modelled by

$$\mathbf{y} = \mathbf{H}\mathbf{x} + \mathbf{n}, \tag{4.10}$$

where $\mathbf{y} \in \mathbb{C}^{K\times 1}$ is the vector that models the received symbols in all receive antennas and $\mathbf{H} = [\mathbf{h}_1; \mathbf{h}_2; \ldots \mathbf{h}_K,] \in \mathbb{C}^{N_t \times K}$ is the channel matrix with $\mathbf{h}_k \in \mathbb{C}^{1\times N_t}$ denoting the channel vector to the kth user, with elements $h_{m,n}$ representing the complex-valued channel coefficient between the nth transmit antenna and the mth receive antenna. Furthermore, $\mathbf{x} \in \mathbb{C}^{N_t \times 1}$ is the vector of precoded transmit symbols that will be discussed in the following and $\mathbf{n} \in \mathbb{C}^{K\times 1} \sim \mathscr{CN}(0, \sigma^2\mathbf{I})$ is the additive white Gaussian noise (AWGN) at the receiver, with $\mathscr{CN}(\mu, \sigma^2)$ denoting the circularly symmetric complex Gaussian distribution associated with a mean of μ and a variance of σ^2.

4.2.1 Closed-Form Precoders, Linear and Non-linear

To accommodate constructive interference the precoding can be designed such that the signal received at the MUs allows for the existence of interference when this is constructive. The first applications of this concept were developed for code division multiple access (CDMA) communications [5, 17–19]. Since then, a number of closed-form precoders have been developed to accommodate constructive interference [6, 12, 20–26] in MU-MISO systems. A generic block diagram of the low-complexity precoding adaptations for a MU-MISO downlink is shown in Fig. 4.6. The essential additional components involve the symbol-by-symbol characterization of interference and the judicious precoding block.

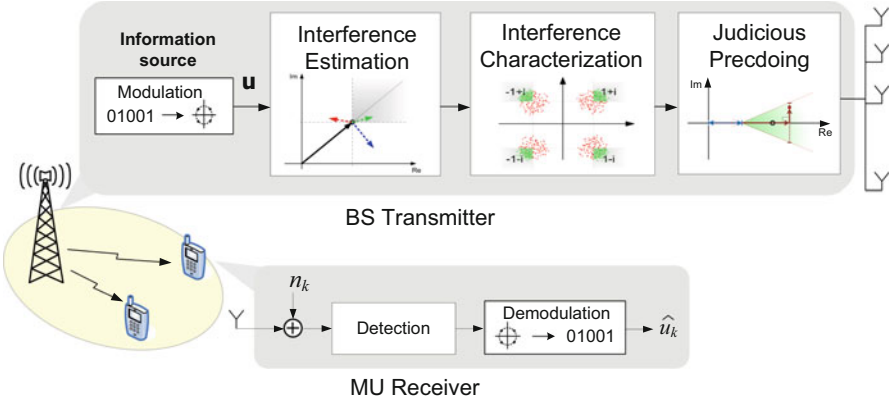

Fig. 4.6 A generic precoding block diagram for the exploitation of interference. Three distinct operations can be observed: interference estimation, interference characterization, and judicious precoding [3]

4.2.1.1 Closed-Form Linear Precoders

Early work such as the one in [6] has looked at adapting simple precoding techniques such as zero forcing (channel inversion) [27] to accommodate for constructive interference in MU-MISO downlinks. Here the main idea is to retain the correlation between the transmitted symbols when it yields constructive interference and eliminate the correlation when it results in destructive interference by means of zero-forcing (ZF) precoding. A further step towards transmitting along interference is shown in [20, 21] for the MU-MISO downlink. Instead of observing and characterizing the interference and zero forcing it accordingly, the precoder actively influences the interference by means of rotational precoding to yield constructive interference. In this case the useful signal benefits from all interfering signals' energy at every symbol period.

To exploit constructive interference the correlation rotation precoder of [20] carefully aligns interference so that it contributes constructively to the desired signal power. In brief, the transmit vectors of [20] follow the typical linear precoding form of

$$\mathbf{x} = \sqrt{\frac{P}{\beta}}\mathbf{W}\mathbf{u}, \tag{4.11}$$

where $\mathbf{u} \in \mathbb{C}^{K\times 1}$ is the modulated data vector, P is the transmit power budget. The precoding matrix $\mathbf{W} = [\mathbf{w}_1, \mathbf{w}_2, \ldots, \mathbf{w}_k] \in \mathbb{C}^{N_t\times K}$, with $\mathbf{w}_k \in \mathbb{C}^{N_t\times 1}$ denoting the beamforming vector for the kth user, is formed as

$$\mathbf{W} = \mathbf{H}^{\dagger}\mathbf{R}_{\phi}, \tag{4.12}$$

where $\mathbf{H}^{\dagger} = \mathbf{H}^H(\mathbf{H}\mathbf{H}^H)^{-1}$ is the Moore–Penrose generalized inverse of the channel matrix, and $\mathbf{R}_{\phi} = \mathbf{R} \odot \mathbf{Q}$, with $\odot$ denoting element-wise matrix multiplication, $\mathbf{R}_{\phi}$ representing the correlation rotation (CR) matrix. The CR matrix contains the elements of the channel correlation matrix $\mathbf{R} = \mathbf{H}\mathbf{H}^H$ rotated by the phase-only matrix $\mathbf{Q}$ with elements in the form $q_{k,l} = e^{j\Delta\phi_{k,l}}$ with

$$\Delta\phi_{k,l} = \angle u_k - \angle u_l\rho_{k,l}, \tag{4.13}$$

such that the resulting interference aligns constructively to the received signal. In (4.13) above, $\rho_{k,l}$ is the k,lth element of the channel correlation matrix $\mathbf{R}$, $\angle x$ denotes the phase of the complex number x. Finally, in (4.11) β is the scaling factor that constraints the average transmit power, and is given as

$$\beta = ||\mathbf{W}||^2 = \text{trace}(\mathbf{W}^H\mathbf{W}). \tag{4.14}$$

Notably, by letting $\mathbf{R}_{\phi} = \mathbf{I}_K$ the CR precoder reduces to the conventional zero-forcing (channel inversion) precoder. It can also be observed that the precoder

in (4.12) combines the channel-only dependent zero-forcing component $\mathbf{H}^{\dagger}$ with the symbol-by-symbol adaptive part in $\mathbf{R}_{\phi}$. By combining (4.10)–(4.12) it can be seen that this results in the following received symbol vector:

$$\mathbf{y} = \sqrt{\frac{P}{\beta}}\mathbf{R}_{\phi}\mathbf{u} + \mathbf{n}, \tag{4.15}$$

where by the definition of matrix $\mathbf{R}_{\phi}$ above, the signal contained in the component $\mathbf{R}_{\phi}\mathbf{u}$ benefits from constructive interference, and falls inside the constructive interference regions in the received constellations, as in Fig. 4.3.

4.2.1.2 Dirty Paper Non-linear Approaches

The capacity achieving alternative to low-complexity linear precoding is dirty paper coding (DPC). While optimal DPC has prohibitive complexity, low-complexity suboptimal approaches have been explored in the form of Tomlinson–Harashima Precoding (THP) [28] and Vector Perturbation (VP) [29]. Both the THP and VP families of techniques have been shown to benefit from harvesting useful signal power from interference.

Interference Optimized Tomlinson–Harashima Precoding THP transmission involves the pre-subtraction of interference at the transmitter in an iterative manner, by which the transmit symbol of the kth user is given as

$$x_k = \left[u_k - \sum_{l=1}^{k-1} b_{k,l} x_l \right] \mathrm{mod}_L \, , k \in [1, K] \tag{4.16}$$

where $b_{k,l}$ is the k,lth element of matrix $\mathbf{B}$, which is the equivalent channel matrix obtained after lower-triangularization, such that each user only sees interference from previously encoded users. u_k is the kth user's information data symbol, selected from an integer constellation $\mathscr{A} = \{\eta^r + i\eta^i | \eta^r, \eta^i \in \{\pm 1, \pm 3, \ldots \pm (\sqrt{M} - 1)\}\}$ where M is the constellation order. Accordingly, THP in (4.16) pre-subtracts from the desired symbol all interference from the previously encoded users. $[.]\mathrm{mod}_L$ denotes the modulo operation with base L, and is used to constrain the transmitted power [28]. Still, this modulo operation results in a transmit power for THP that is higher compared to uncoded transmission, a situation referred to as *Power Loss*.

A number of adaptations of THP have been developed such that interference is exploited to improve the interference pre-subtraction function of the THP encoder. Interference-optimized THP (IO-THP) in [30, 31] exploits the power of interference to reduce the abovementioned power loss. It uses an encoding strategy where the amplitude and phase of the useful signal for a number of users is optimized, within the constructive constellation sectors as shown in Fig. 4.3 and under an SNR

threshold, such that the resulting interference is better aligned to the symbols of interest. In this way the power required by THP encoding to subtract the interference (and therefore the transmitted power) is minimized, leading to a more power-efficient transmission. Accordingly, for IO-THP the data symbols for a subset $K_s \leq K$ users are scaled by the real-valued factors v_k^r, v_k^i as

$$\tilde{u}_k = v_k^r u_k^r + i v_k^r u_k^i, \; k \in [1, K_s] \tag{4.17}$$

where $u_k^r = \text{Re}(u_k), u_k^i = \text{Im}(u_k)$, and v_k^r, v_k^i are carefully optimized such that $\tilde{u}_k$ falls in the constructive area of the modulation constellation as discussed in the previous section and shown in Fig. 4.3. Thereafter, the typical THP pre-subtraction is applied to the modified data symbols as

$$\tilde{x}_k = \left[\tilde{u}_k - \sum_{l=1}^{k-1} b_{k,l} \tilde{x}_l(v^*) \right] \text{mod}_L, k \in [1, K] \tag{4.18}$$

where now the transmitted symbols $\tilde{x}_k$ are a function of the optimal scaling factors v^*. For the details of the optimization of the factors v_k^r, v_k^i the reader is referred to [30, 31]. By means of the above constructive symbol optimization, power is saved from the interference-cancellation operation and invested in the useful signal as a source of additional signal power.

An illustrative result of this effect is shown in Fig. 4.7 where the performance in terms of bit error rate (BER) is shown for a system with $N_t = 4, K = 4$ as a function of the transmit power in vector $\mathbf{x}$ expressed as the percentage of the power of the uncoded symbols in vector $\mathbf{u}$, for conventional THP and IO-THP with increasing numbers of prescaled users K_s. A trade-off between transmit power and performance can be obtained for IO-THP by varying the SNR threshold involved in the optimization of the pre-scaling factors [30, 31]. While in this chapter we skip the details of this trade-off, the main message in this result is that, by harvesting the interference energy in this scenario, IO-THP achieves a transmit power reduction down to $1/6$ of that for conventional THP, for the same BER performance.

Constructive Vector Perturbation Precoding Vector perturbation designates another family of non-linear precoders that employ a channel inversion precoding matrix and apply a perturbation on the transmitted symbols such that the signal content at the receiver is maximized. The transmitted signal is given by [29]

$$\mathbf{x} = \sqrt{\frac{P}{\beta}} \mathbf{H}^\dagger (\mathbf{u} + \tau \mathbf{l}^\star) \tag{4.19}$$

where

$$\beta = ||\mathbf{H}^\dagger (\mathbf{u} + \tau \mathbf{l}^\star)||^2 \tag{4.20}$$

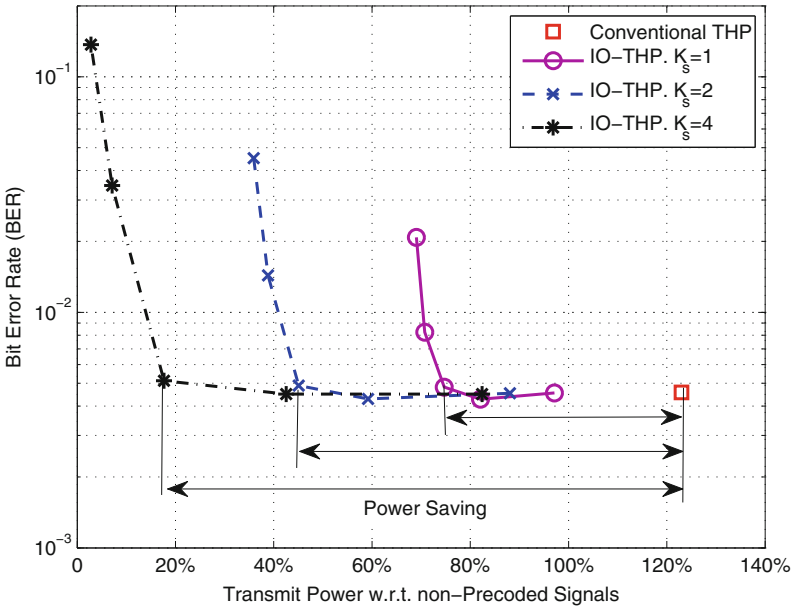

Fig. 4.7 BER versus transmit power for THP, and IO-THP. $N_t = K = 4$, QPSK, SNR $= 29$ dB [31]

is the transmit power scaling factor so that $||\mathbf{x}||^2 = P$ and $\mathbf{l}^\star \in \mathbb{C}^{M\times 1}$ is the selected perturbation vector with integer entries. Also $\tau = 2|c|_{\max} + \Delta$ where $|c|_{\max}$ is the absolute value of the constellation symbol with the maximum magnitude and Δ denotes the minimum Euclidean distance between constellation symbols. The idea here is that the perturbation vectors $\mathbf{l}^\star$ are introduced to increase the degrees of freedom in optimizing the resulting performance, and are later removed at the receiver by applying a modulo operation with base τ.

Accordingly, the perturbation vectors $\mathbf{l}^\star$ are chosen from an integer constellation $\mathbb{Z}^M + j\mathbb{Z}^M$ to maximize the signal component in the received symbols or equivalently minimize β and the resulting the noise amplification at the receiver, as

$$\mathbf{l}^\star = \arg \min_{\mathbf{l}\in\mathbb{Z}^M + j\mathbb{Z}^M} ||\mathbf{H}^\dagger(\mathbf{u} + \tau\mathbf{l})||^2 \tag{4.21}$$

This is typically an NP hard problem solved with sphere search techniques [32] that have complexity which grows exponentially with the number of users K.

To apply the concept of interference exploitation, the above optimization can be constrained to ensure that the perturbation vectors add up strictly constructively to the information symbols, so that the removal of perturbation is not necessary at the receiver and the receiver complexity can be drastically reduced. In particular, in the constructive vector perturbation approach of [33] the search space for the

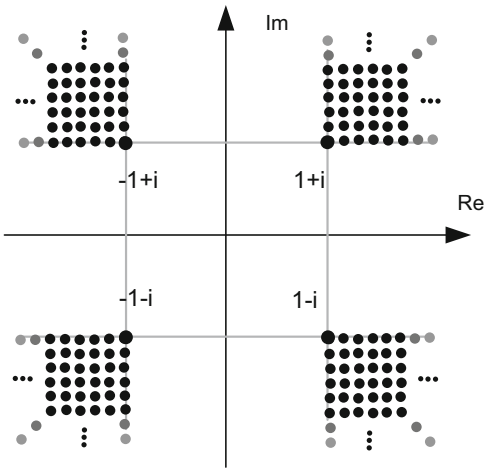

Fig. 4.8 Constructive perturbation lattice, QPSK example [30]

perturbation vectors is limited to the constructive areas in the symbol constellation. In other words the above optimization is modified (4.21) to

$$\mathbf{l}^{\star} = \arg\min_{\mathbf{l}\in\mathbb{A}^M} ||\mathbf{H}^{\dagger}(\mathbf{u} + \tau\mathbf{l})||^2 \tag{4.22}$$

where $\mathbb{A}^M$ is a lattice that only involves the constructive areas of the constellation as shown in Fig. 4.3. For the example of QPSK this constellation can be described as $\mathbb{A}^M = \left\{0, \varepsilon\left(m \cdot \text{sgn}\{\text{Re}(\mathbf{u})\} + n \cdot \text{sgn}\{\text{Im}(\mathbf{u})\}\right)\right\}$ where $m, n \in \{1, 2, 3 \ldots\}$, sgn$\{x\}$ denotes the sign of x and ε is an arbitrary constant, which results in the lattice shown in Fig. 4.8. The effect of this optimization is that, as the perturbed signals lie in the constructive areas of the constellation, there is no need to remove the perturbation at the receiver, which therefore alleviates the need to apply the $[.]\text{mod}_{\tau}$ operation at the receiver and the need to feed-forward the scaling factor β for receiver equalization. This further implies that there is no need for the perturbation quantities to take integer values, and in fact, it is shown in [33] that the perturbation operation can be transformed into a linear scaling operation in the form

$$\mathbf{x} = \sqrt{\frac{P}{\beta}}\mathbf{H}^{\dagger}\mathbf{S}\mathbf{u} \tag{4.23}$$

where $\mathbf{S}$ is a diagonal scaling matrix with elements s_i and $\beta = ||\mathbf{H}^{\dagger}\mathbf{S}\mathbf{u}||^2$. Accordingly, the perturbation search need not apply on an integer lattice $\mathbb{A}^M$ like the one in (4.21), (4.22), and can be extended to all points in the constructive regions of the symbols' constellation. By applying a lower-threshold s_t on the scaling factors so that a minimum QoS level is guaranteed, the perturbation search can be transformed into

$$\mathbf{S}^{\star} = \arg\min_{\mathbf{S}} ||\mathbf{H}^{\dagger}\mathbf{S}\mathbf{u}||^2$$
$$\text{s.t.} \quad s_i \geq s_t, \forall i \tag{4.24}$$

that can be solved with quadratic programming. As a result, it has been shown that this can offer up to an order of magnitude complexity reduction at the transmitter for a moderate MU-MISO downlink with $N_t = 10, K = 10$ [33].

4.2.2 *Beamforming Optimization for Constructive Interference*

The above early work on closed-form precoders has been the baseline for designing a number of optimum beamforming designs, specifically tailored for accommodating and maximizing constructive interference. These have built upon traditional optimization techniques that directly minimize the transmit power subject to quality of service (QoS) constraints—most commonly the signal-to-interference-plus-noise ratio (SINR)—for the MU-MISO downlink [34], where convex optimization strategies are typically pursued. Moreover, SINR balancing optimizations [35] are of interest, where the minimum achievable SINR is maximized, subject to a total transmit power constraint. In all these strategies, from a stochastic point of view and treating interference as harmful, the average SINR for the ith user is typically expressed as

$$\gamma_i = \frac{|\mathbf{h}_i\mathbf{w}_i|^2}{\sum_{k=1,k\neq i}|\mathbf{h}_i\mathbf{w}_k|^2 + N_0} \tag{4.25}$$

where $\mathbf{h}_i$ and $\mathbf{w}_i$ are the channel vector and the beamforming vector for the ith user, and N_0 is the noise spectral density.

Power Minimization The conventional power minimization precoder, treating all interference as harmful, aims to minimize the average transmit power subject to an SINR threshold Γ_i by formulating the optimization problem shown below [34]

$$\min_{\{\mathbf{w}_i\}} \sum_{i=1}^{K} \|\mathbf{w}_i\|^2 \tag{4.26}$$
$$\text{s.t.} \quad \frac{|\mathbf{h}_i\mathbf{w}_i|^2}{\sum_{k=1,k\neq i}|\mathbf{h}_i\mathbf{w}_k|^2 + N_0} \geq \Gamma_i, \forall i.$$

The above optimization is most commonly solved as a second-order cone programming (SOCP) problem or exploiting uplink/downlink duality [34].

SINR Balancing SINR balancing maximizes the minimum achievable SINR subject to a transmit power budget, in the form

$$\begin{aligned} \max_{\mathbf{w}_w} \quad & \Gamma_t \\ \text{s.t.} \quad & \frac{\|\mathbf{h}_i \mathbf{w}_i\|^2}{\sum_{k=1,k\neq i} \|\mathbf{h}_i \mathbf{w}_k\|^2 + N_0} \geq \Gamma_t, \forall i. \\ & \sum_{i=1}^{K} \|\mathbf{w}_i\|^2 \leq P \end{aligned} \tag{4.27}$$

where P denotes the total transmit power budget. We note that the above optimization is non-convex and the solution involves more complex iterative approaches [35].

4.2.2.1 Beamforming for Interference Exploitation

By harvesting useful signal power from constructive interference, recent works in the area of beamforming optimization [8, 36–39] have shown significant gains with respect to the above optimization. Specifically, it has been demonstrated that the transmit power required for a given QoS threshold can be drastically reduced in the power minimization problem, or equivalently the QoS obtained for a given transmit power can be drastically improved in the SINR balancing formulation. More recently, these beamforming strategies have been extended to the realm of hybrid analog-digital precoding, to exploit mutual coupling between the transmit antennas by means of tunable antenna loads [40].

Let us place our attention on how the beamforming optimization can be adapted to exploit constructive interference. As per the interference classification and discussion in Sect. 4.1.2, the optimizations in (4.26), (4.27) can be modified to take the constructive interference into account. This can be done by imposing interference constraints, not in terms of suppressing the stochastic interference, but rather optimizing instantaneous interference to contribute to the received signal power, thus providing a source for harvesting useful signal power. Indeed, for the case when interference has been aligned, by means of precoding vectors $\mathbf{w}_k$, to overlap constructively with the signal of interest, all interference in the received signal contributes constructively to the useful signal. Accordingly, it has been shown in [20] that in this case the instantaneous received SNR is given as

$$\gamma_i = \frac{\left|\mathbf{h}_i \sum_{k=1}^{K} \mathbf{w}_k u_k\right|^2}{N_0} \tag{4.28}$$

where all interference contributes in the useful received signal power.

Strict Phase Alignment Accordingly, and based on the classification criteria detailed in [5] and Fig. 4.3 for constructive interference, the first approach in this area in [36], focusing on PSK modulation in the form $u_i = e^{j\phi_i}$, introduced

a modified interference constraint in (4.26) where interference is constrained to strictly align to the phase of the useful signal. The power minimization problem was reformulated in [36] as

$$\begin{aligned} \min_{\{\mathbf{w}_i\}} \quad & \left\| \sum_{k=1}^{K} \mathbf{w}_k e^{j(\phi_k - \phi_i)} \right\|^2 \\ \text{s.t.} \quad & \angle \left(\mathbf{h}_i \sum_{k=1}^{K} \mathbf{w}_k u_k \right) = \angle(u_i), \forall i \\ & \text{Re} \left(\mathbf{h}_i \sum_{k=1}^{K} \mathbf{w}_k e^{j(\phi_k - \phi_i)} \right) \geq \sqrt{\Gamma_i N_0}, \forall i. \end{aligned} \tag{4.29}$$

Here clearly the transmit power is minimized on an instantaneous basis in the objective function, and the first set of constraints imposes that, for each user, the phase of interference is strictly constrained to equal the phase of the symbol of interest. The second set of constraints poses QoS constraints for each user, in the form of the SNR thresholds Γ_i which relate to the instantaneous SNR expression in (4.28).

We note the use of the sum of phase shifted (by the phase of the symbol of interest ϕ_i) interfering symbols plus the symbol of interest in the above expressions. This is in line with our analysis above in Sect. 4.1.2, and serves to isolate the received amplitude and phase shift in the symbol of interest due to interference. Note that the above two conditions contain K equations and K inequalities, while there are $2N_t \geq 2K$ real variables, so there are sufficient degrees of freedom to satisfy these two sets of constraints.

Phase Relaxation Still, it can be seen that due to the strict angle constraint, the formulation (4.29) is more constrained than the constructive interference regions in Fig. 4.3 where the strict phase constraints do not exist. To obtain a more relaxed optimization for M-PSK, we resort to the previous classification criteria in Sect. 4.1.2 which we extend to incorporate an arbitrary SNR constraint γ. With reference to Fig. 4.4, and using the beamforming vectors $\mathbf{w}_k$ the above-defined components of the phase rotated received symbols excluding interference can be rewritten as

$$\alpha_R = \text{Re} \left(\mathbf{h}_i \sum_{k=1}^{K} \mathbf{w}_k e^{j(\phi_k - \phi_i)} \right), \text{ and } \alpha_I = \text{Im} \left(\mathbf{h}_i \sum_{k=1}^{K} \mathbf{w}_k e^{j(\phi_k - \phi_i)} \right) \tag{4.30}$$

To extend the above discussion to the case where constructive interference is defined with respect to an SNR threshold—as opposed to the nominal constellation points—let us look at Fig. 4.9 where we have revisited the geometry of Fig. 4.4 by

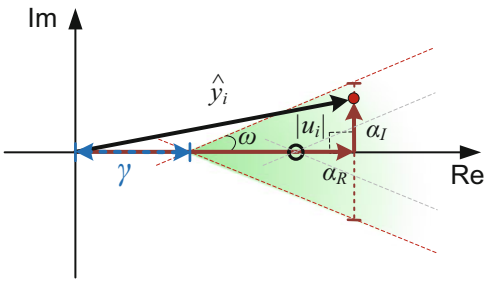

Fig. 4.9 Optimization region for beamforming for interference exploitation based on SNR threshold γ

introducing an SNR parameter $\gamma = \sqrt{\Gamma_i N_0}$, following the SNR expression (4.28). This gives rise to the constructive interference sector denoted by the green shaded sector in Fig. 4.9. By a similar process to that in Fig. 4.4 it can be seen that α_R and α_I are allowed to grow infinitely, as long as their ratio is such that the received symbol is contained within the constructive area of the constellation, i.e., the distances from the decision boundaries, as set by the SNR constraints Γ_i, are not violated. Accordingly, α_R, α_I have to follow

$$|\alpha_I| \leq \left(\alpha_R - \gamma\right) \tan \omega \tag{4.31}$$

As regards the constructive area in the constellation, with respect to (4.29), it can be seen that the angle of the received signal need not strictly align with the angle of the useful signal, as long as it falls within the constructive area of the constellation with a maximum phase shift of $\Delta\phi = \pm\pi/M$, for an M-PSK modulation. Accordingly, to relax the optimization, α_I is allowed to be non-zero as long as the resulting symbol lies within the constructive area of the constellation.

Power Minimization with Interference Exploitation Using (4.30), (4.31) we arrive at the power minimization problem presented in [37] as

$$\begin{aligned} &\min_{\{\mathbf{w}_i\}} \left\| \sum_{k=1}^{K} \mathbf{w}_k e^{j(\phi_k - \phi_i)} \right\|^2 \\ &\text{s.t.} \left| \text{Im}\left(\mathbf{h}_i \sum_{k=1}^{K} \mathbf{w}_k e^{j(\phi_k - \phi_i)} \right) \right| \leq \left(\text{Re}\left(\mathbf{h}_i \sum_{k=1}^{K} \mathbf{w}_k e^{j(\phi_k - \phi_i)} \right) - \sqrt{\Gamma_i N_0} \right) \tan \omega, \forall i \end{aligned} \tag{4.32}$$

It can be seen that the above optimization in (4.32) is more relaxed than the zero-angle-shift optimization (4.29), which results in a smaller minimum in the transmit power. Moreover, it contains a number of K inequalities which result in an increased feasibility region compared to the conventional optimization, as detailed

in [37]. Problem (4.32) is a standard second-order cone program (SOCP), thus can be optimally solved using numerical software.

SNR Balancing with Interference Exploitation The respective SNR balancing problem that allows interference exploitation can be designed in a similar fashion as

$$\begin{aligned} &\max_{\{\mathbf{w}_i\}} \ \Gamma_t \\ &\text{s.t.} \ \left| \text{Im}\left(\mathbf{h}_i \sum_{k=1}^{K} \mathbf{w}_k e^{j(\phi_k - \phi_i)} \right) \right| \leq \left(\text{Re}\left(\mathbf{h}_i \sum_{k=1}^{K} \mathbf{w}_k e^{j(\phi_k - \phi_i)} \right) - \sqrt{\Gamma_t N_0} \right) \tan\omega, \forall i \\ &\left\| \sum_{k=1}^{K} \mathbf{w}_k e^{j(\phi_k - \phi_i)} \right\|^2 \leq P \end{aligned} \tag{4.33}$$

Remarkably, the relaxed nature of the interference-exploitation beamforming problems leads to larger feasibility regions. To illustrate the extended feasibility region for the optimization problems (4.32), (4.33), Fig. 4.10 shows the feasibility probability of a $K = 4$ user system with respect to the number of transmit

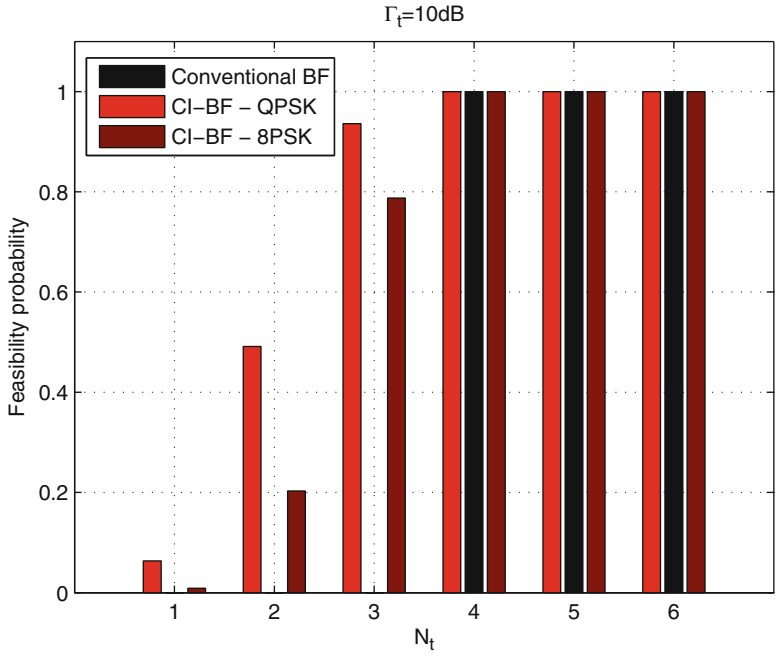

Fig. 4.10 Feasibility probability vs. N_t for conventional and interference-exploitation beamforming, $K = 4$, $\Gamma_t = 10$ dB [37]

antennas N_t. The comparison is between the conventional beamforming of (4.26) ("Conventional BF" in the legend) and the constructive interference beamforming of (4.32) ("CI-BF") for the cases of QPSK and 8PSK modulation. It can be seen that, while the conventional optimization is only feasible for $N_t \geq K$, the proposed can be feasible with non-zero probability for lower values of N_t. This observation could have a significant impact in the communication system design, where, by applying interference-exploitation principles, more users can be scheduled simultaneously in a given cell. Furthermore, it is important to note that the cell-edge users are more prone to interference. In a single cell scenario this would be naturally captured and exploited with the above interference-exploitation optimizations, given the channel characteristics. More importantly, regarding other-cell interference, this is the topic of multi-cell interference exploitation, which while captured to-date in CR applications [13–16], is a widely open research area in the context of interference exploitation.

Beamforming Optimizations for QAM Constellations While the above approaches are shown for PSK constellations, the works in [8, 9] and more recently in [10–12] have applied the interference-exploitation beamforming approaches to QAM and star-QAM modulations. This has been pursued by adapting the interference constraints in the beamforming optimizations according to the interference classification for QAM constellations outlined in Sect. 4.1.2 and in (4.9). The keen reader is referred to [10, 11] for detailed formulations of the corresponding optimizations.

Notably, all the above interference-exploitation optimizations allow for equivalent multicast formulations to be employed, which result in more efficient solvers with much reduced complexity, as detailed in [36, 37]. Still, it is clear that the interference-exploitation beamformers are data dependent and therefore require the optimization problem to be solved on a symbol-by-symbol basis. This therefore necessitates a closer look at the resulting complexity.

4.2.2.2 Notes on the Complexity of Interference-Exploitation Beamforming

To facilitate the complexity comparison, the main signal-processing operations for the conventional and the interference-exploitation beamforming approaches are illustrated in the block diagrams of Fig. 4.11a, b, respectively.

Transmit (Base Station) Complexity With the low-complexity multicasting simplifications derived in [36, 37] it has been shown that the complexity of solving the equivalent multicasting optimization problems of (4.32), (4.33) is greatly reduced. In fact, the complexity study found in [37] has shown that, due to the relaxed nature of the problem, computationally efficient gradient projection approaches can be developed that achieve a complexity of down to 15% w.r.t. conventional power minimization precoding, for each precoding optimization. More recent work in [39] relying on barrier-method solvers has further reduced the complexity down

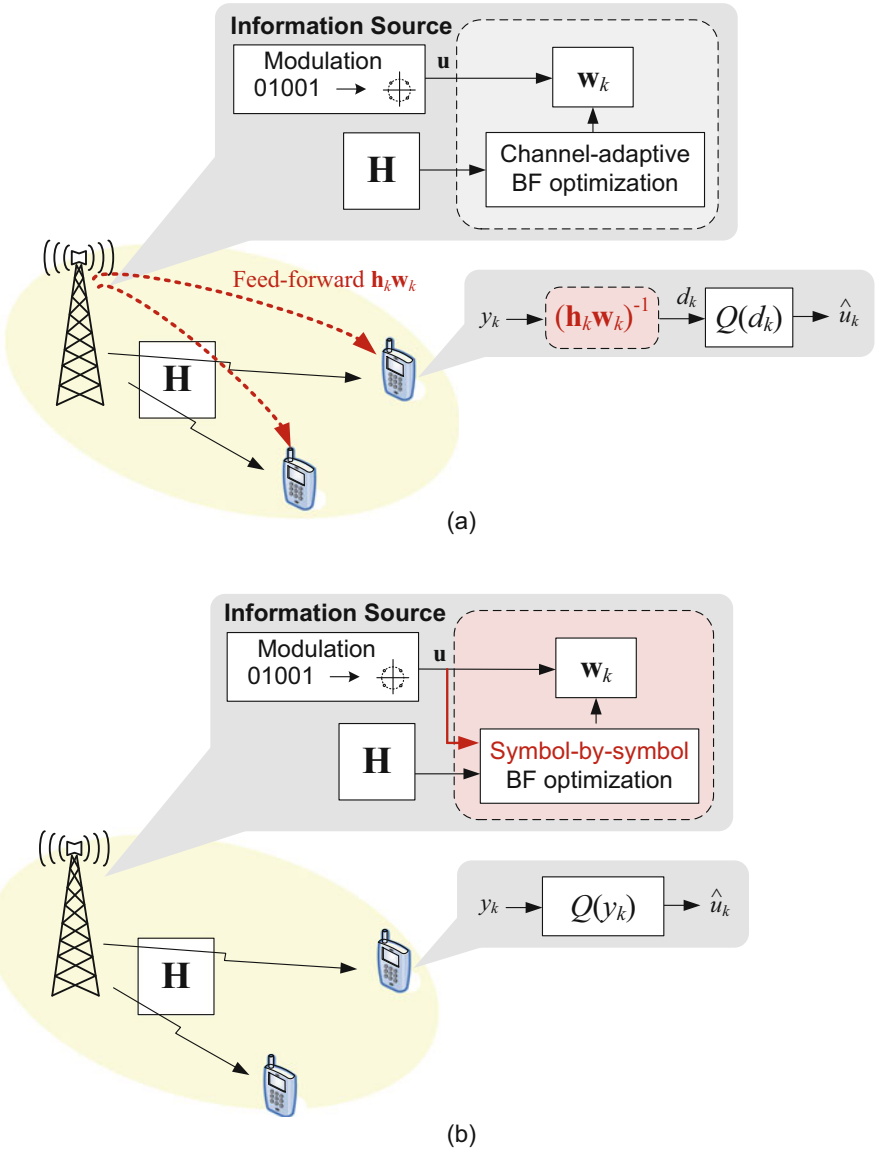

Fig. 4.11 Block diagram showing transmit and receive processing, (**a**) conventional beamforming optimization, (**b**) beamforming for interference exploitation

to 2% w.r.t. conventional beamforming. However, as the interference-exploitation beamforming optimizations need to be performed on a symbol-by-symbol basis (denoted in the red box in Fig. 4.11b), a frame-based complexity analysis is pertinent. For the example of an LTE Type 2 TDD frame with up to 112 downlink

symbol time slots [7], this translates to a doubling of complexity per frame of $112 \times 2\% = 224\%$ for the interference-exploitation schemes w.r.t. conventional precoding optimization. It is important to note that this complexity involves the base station (BS) transmitter, where computational resources are more accessible. At the same time, the complexity of the mobile units is drastically reduced as explained below. In addition, this complexity increase comes with significant power savings of, for example, up to 3 dB for a small scale MU-MISO downlink of $N_t = 4, K = 4$ [37].

Power Efficiency In fact, in terms of the ultimate metric of power efficiency at the transmitter, for an LTE base station the transmit power is typically measured on the order of 20 W, while the power consumption of the DSP processing is typically orders of magnitude lower. Since with the interference-exploitation beamformers show a halving of the transmit power at roughly double the DSP power w.r.t. to their conventional counterparts, the gains in the power efficiency by harvesting useful signal power form interference are therefore undeniable.

Receiver (Mobile Unit) Complexity Regarding the receive complexity, the proposed approaches provide significant benefits compared to conventional beamforming. Indeed, for conventional beamforming the MU receiver is required to equalize the composite channel $\mathbf{h}_i\mathbf{w}_i$ from (4.26), (4.27) as shown in the red box in Fig. 4.11a, in order to recover the data. This necessitates that the BS feed-forward the composite channel to each MU receiver for correct detection, denoted by the dashed red arrows in Fig. 4.11a. Clearly, this is subject to CSI quantization and detection errors, and introduces additional computational overheads at the MU receivers.

By contrast, as for the interference-exploitation approaches the received symbols lie at the constructive area of the constellation (see Fig. 4.3), there is no need for equalizing the composite channel $\mathbf{h}_i\mathbf{w}_i$ to recover the data symbols at the ith MU, and a simple decision stage suffices. Accordingly, the benefit of interference-exploitation approaches is that CSI is not required for detection at the MU, which allows for significant savings in the training time and computational overheads for signalling the beamformers to the MUs. It also makes these schemes immune to the quantization errors involved in the feed-forward of $\mathbf{h}_i\mathbf{w}_i$ for conventional beamforming. The resulting benefits are quantified in [15].

4.2.3 Resource Allocation for Interference Exploitation

The gains obtained by the above adaptations can be augmented by employing specifically tailored resource allocation techniques. To enhance the performance of the interference-exploitation schemes the goal of resource allocation would be, instead of allocating resources that inherently experience minimum interference, to optimize the interference between the resources according to QoS criteria.

This of course covers a vast area where resources can pertain to antenna selection, power allocation, sub-carrier allocation in OFDM, user association and scheduling,

and so on. In this subsection, we overview recent antenna selection [41–43] and power allocation [25] strategies developed to optimize and exploit constructive interference, while the same concept can be extended to alternative resources such as user scheduling [44], adaptive modulation [11], or specific power allocation for non-orthogonal multiple access (NOMA) [45] combined with interference exploitation. Building upon the power allocation work, we further look at constant envelope precoding (CEP) [46] where the CEP is optimized to exploit constructive interference under given per-antenna power budgets.

4.2.3.1 Antenna Selection

The antenna-selection techniques developed for interference exploitation build upon existing antenna-selection benchmark schemes, namely capacity maximization [47] and path gain selection [48].

Capacity Maximization Recent work in the area of large scale antenna systems [49] showed channel-capacity-based antenna selection can be performed by means of convex optimization, drastically reducing the complexity of previous techniques from the literature, such as the capacity maximization technique in [50]. Accordingly, the selection of N_s antennas out of the available N_t antennas at the transmitter is performed over the system sum-capacity, and the optimization problem is formulated as

$$\begin{aligned} \max_{\boldsymbol{\Delta}} \ & \log_2 \left[\det \left(\mathbf{I}_K + \zeta \mathbf{H}^H \boldsymbol{\Delta} \mathbf{H} \right) \right] \\ \text{s.t.} \ & \Delta_{n,n} \in [0,1], \\ & \textstyle\sum_{n=1}^{N} \Delta_{n,n} = N_s. \end{aligned} \tag{4.34}$$

where ζ is an SNR parameter and $\boldsymbol{\Delta}$ is an $N_t \times N_t$ selection matrix. In particular, $\boldsymbol{\Delta}$ is a real diagonal matrix, whose entries should be either null, i.e., $\Delta_{n,n} = 0$ if n is a non-selected antenna, or unitary, i.e., $\Delta_{n,n} = 1$ if n is an antenna selected for transmission. Since constraining the diagonal values of $\boldsymbol{\Delta}$ to be binary results in a non-convex formulation, a relaxation such that the elements of $\boldsymbol{\Delta}$ take values in between 0 and 1, i.e., $\Delta_{n,n} \in \{0, 1\}$ in the optimization (4.34) above is commonly adopted. With the above relaxation, the optimization problem becomes convex, and the final selection can be done by rounding the elements such that $\Delta_{n,n} \in [0, 1]$. This approach has been shown to achieve near-optimal performance in the large scale MIMO regime when compared to exhaustive search approaches [47].

Path Gain Selection A similar approach selects the subset of antennas whose path gains are higher, according to the following optimization:

$$\begin{aligned} \max_{\boldsymbol{\Delta}} \ & \mathbf{H}^H \boldsymbol{\Delta} \mathbf{H} \\ \text{s.t.} \ & \Delta_{n,n} \in \{0,1\}, \\ & \textstyle\sum_{n=1}^{N} \Delta_{n,n} = N_s. \end{aligned} \tag{4.35}$$

This form of selection has received a lot of attention due to its simplicity.

4.2.3.2 Antenna Selection for Interference Exploitation

Given the conditions for constructive interference reviewed in the previous sections, it is possible to identify new antenna-selection metrics that maximize constructive interference, thus optimally exploiting this important source of useful signal power.

Antenna Selection for Closed-Form Precoding Initial approaches were introduced in [41, 42] where the selection takes place for given closed-form precoding vectors $\mathbf{w}_k$ such as selective precoding (SP) [41], matched filtering (MF), or correlation rotation (CR) [42]. In the more recent work of [42], the problem was formulated as

$$\begin{aligned} \max_{\boldsymbol{\Delta}} \min_{i} \ & \left(\mathrm{Re}\left(\mathbf{h}_i \boldsymbol{\Delta} \textstyle\sum_{k=1}^{K} \mathbf{w}_k e^{j(\phi_k - \phi_i)} \right) \right) \tan\omega - \left| \mathrm{Im}\left(\mathbf{h}_i \boldsymbol{\Delta} \textstyle\sum_{k=1}^{K} \mathbf{w}_k e^{j(\phi_k - \phi_i)} \right) \right| \\ \text{s.t.} \ & \Delta_{n,n} \in \{0,1\}, \\ & \textstyle\sum_{n=1}^{N} \Delta_{n,n} = N_s. \end{aligned} \tag{4.36}$$

The above optimization selects the antenna subset that maximizes the minimum constructive interference amongst the users for a given set of $\mathbf{w}_k$ in the MU-MISO downlink. The above approach is most suitable for large scale antenna systems with a low-complexity MF precoder and with a sufficient number of transmit antennas that guarantee constructive interference for all users. A clear connection to the interference-exploitation beamforming optimizations in the previous section can be seen, with the addition of the selection matrix $\boldsymbol{\Delta}$, along with the antenna-selection constraints.

Joint Antenna Selection and Precoding Optimization Going one step further, the approach in [43] pursues a joint optimization of both the antenna subset and the precoding vectors, by formulating the problem as

$$\begin{aligned} \max_{\boldsymbol{\Delta}, \{\mathbf{w}_i\}} \min_{i} \ & \left(\mathrm{Re}\left(\mathbf{h}_i \boldsymbol{\Delta} \textstyle\sum_{k=1}^{K} \mathbf{w}_k e^{j(\phi_k - \phi_i)} \right) \right) \tan\omega - \left| \mathrm{Im}\left(\mathbf{h}_i \boldsymbol{\Delta} \textstyle\sum_{k=1}^{K} \mathbf{w}_k e^{j(\phi_k - \phi_i)} \right) \right| \\ \text{s.t.} \ & \Delta_{n,n} \in \{0,1\}, \\ & \textstyle\sum_{n=1}^{N} \Delta_{n,n} = N_s, \\ & \left\| \textstyle\sum_{k=1}^{K} \mathbf{w}_k e^{j(\phi_k - \phi_i)} \right\|^2 \leq P. \end{aligned} \tag{4.37}$$

As we can see, the above formulation is designed to jointly optimize the antenna selection by means of $\boldsymbol{\Delta}$, together with the precoding vectors $\mathbf{w}_i$. The joint optimization allows us to fully exploit the resulting constructive interference, and can be solved using mixed integer programming techniques [51].

Successive Optimization To reduce the optimization complexity, the above problem can be decomposed into two sub-problems and solved with a successive optimization approach. In [43] first a subset selection is performed by solving the following optimization problem based on the antenna cross-correlations $\mathbf{h}_i\mathbf{h}_k^H$:

$$\begin{aligned} \max_{\boldsymbol{\Delta}} \min_{i} \; & \left(\mathrm{Re}\left(\mathbf{H}^H \boldsymbol{\Delta} \mathbf{H} e^{j\boldsymbol{\phi}-\phi_i}\right)\right) \tan\omega - \left|\mathrm{Im}\left(\mathbf{H}^H \boldsymbol{\Delta} \mathbf{H} e^{j\boldsymbol{\phi}-\phi_i}\right)\right| \\ \text{s.t.} \quad & \Delta_{n,n} \in \{0,1\}, \\ & \textstyle\sum_{n=1}^{N} \Delta_{n,n} = N_s. \end{aligned} \tag{4.38}$$

where $\boldsymbol{\phi} = [\phi_1, \phi_2, \ldots, \phi_i]^T$. It can be observed that the above bears resemblance to the path gain selection of (4.35), but with a modified objective function, specifically tailored for constructive interference. Then, for the selected subset of antennas corresponding to the channel matrix $\tilde{\mathbf{H}} = [\tilde{\mathbf{h}}_1; \tilde{\mathbf{h}}_2; \ldots; \tilde{\mathbf{h}}_K]$, the optimal precoding vectors $\mathbf{w}_k$ are computed by solving the following problem:

$$\begin{aligned} \max_{\{\mathbf{w}_i\}} \min_{i} \; & \left(\mathrm{Re}\left(\tilde{\mathbf{h}}_i \textstyle\sum_{k=1}^{K} \mathbf{w}_k e^{j(\phi_k-\phi_i)}\right)\right) \tan\omega - \left|\mathrm{Im}\left(\tilde{\mathbf{h}}_i \textstyle\sum_{k=1}^{K} \mathbf{w}_k e^{j(\phi_k-\phi_i)}\right)\right| \\ \text{s.t.} \quad & \left\| \textstyle\sum_{k=1}^{K} \mathbf{w}_k e^{j(\phi_k-\phi_i)} \right\|^2 \leq P. \end{aligned} \tag{4.39}$$

which is now a function of $\mathbf{w}_i$ only. Both max–min optimizations in (4.38), (4.39) are convex and can be solved using an auxiliary threshold variable as, for example, in (4.27). It has been shown in [43] that the successive optimization approach in (4.38), (4.39) performs within 0.5 dB of the joint optimization approach of (4.37), at a significantly reduced complexity, down to $1/6$ of the joint optimization complexity for a large scale system with $N_t = 128, K = 5$. It can be observed in the relevant works that both beamforming and antenna selection for interference exploitation provide significant performance benefits. Whether the former or the latter are dominant in a practical scenario is subject to the size of the system and the number of auxiliary antennas.

4.2.3.3 Power Allocation for Constructive Interference Maximization

Power allocation approaches in the area of interference exploitation have mainly focused on the closed-form precoders of Sect. 4.2.1. Firstly, it is important to note that, contrary to conventional zero-forcing precoding, the precoders in [12, 20–25] do not obtain uniform performance across all users. This is because the power of

constructive interference received may vary from user to user. Building on this observation, an interesting power allocation approach in [25], designed for CR precoding, optimizes the power allocation amongst the users such that the worst user's SNR is maximized. First it is shown that the user with the worst SNR is the one that experiences the minimum constructive interference, which for CR is measured by the parameter

$$c_i = \sum_{k=1}^{K} |\rho_{i,k}| \tag{4.40}$$

where $\rho_{i,k}$ is the i,kth element of the channel correlation matrix as defined in Sect. 4.2.1. Accordingly, the per-user power p_i is determined by solving the following optimization:

$$\begin{aligned} &\max_{\{p_i\}} \min_i \; c_i^2 p_i \\ &\text{s.t.} \qquad \sum_i p_i = P_T, 0 \le p_i \end{aligned} \tag{4.41}$$

where P_T is the total transmit power budget. It can be seen that the above power allocation ensures the same SINR to all users, which constitutes an SINR balancing approach.

4.2.3.4 Constructive Constant Envelope Precoding

Constant envelope precoding (CEP), where the amplitude of the transmitted symbols remains unchanged, has received particular attention recently due to its suitability for large scale antenna systems envisaged for 5G implementations.

Building on the above power allocation discussion, and given a per-antenna transmit power budget P_n for the nth transmit antenna, CEP forms the transmitted symbol from the nth antenna of the BS as [52]

$$x_n = \sqrt{P_n} e^{j\theta_n}, \tag{4.42}$$

where θ_n represents the precoding phase of the CEP signal. It is clear that the transmitted symbols have a constant envelope of $\sqrt{P_n}$ with phase-only variation. For notational simplicity, let us assume that all transmit antennas obey $P_n = \frac{1}{N_t}, \forall n \in \{1, \ldots, N_t\}$, in which case we can write

$$\mathbf{x} = \frac{1}{\sqrt{N_t}} e^{j\boldsymbol{\theta}}, \tag{4.43}$$

where $\boldsymbol{\theta} = [\theta_1, \theta_2, \ldots, \theta_{N_t}]^T$. Accordingly CEP aims at minimizing the interference as [52]

$$\begin{aligned} &\min_{\boldsymbol{\theta}} \sum_{m=1}^{M} \left| \tfrac{1}{\sqrt{N_t}} \mathbf{h}_m e^{j\boldsymbol{\theta}} - u_m \right|^2 \\ &\text{s.t. } |\theta_n| \leq \pi, \forall n \in \{1, \ldots, N_t\}, \end{aligned} \tag{4.44}$$

where, unlike the transmit symbols x_n, the information symbols u_n can be taken from a constellation with either constant or non-constant envelope. The above optimization represents a non-convex non-linear least squares (NLS) problem, subject to local minima. The optimization problem (4.44) was first solved in [52] with a gradient descent (GD) based approach, and further improved in [53] with a direct application of the cross-entropy method [54].

Constructive CEP Exploiting the concept of constructive interference in Sect. 4.1.2, it is possible to define a new optimization problem that maximizes the constructive interference, while employing phase-only transmit symbols. Accordingly, in [46] the CEP optimization problem was defined for PSK symbols $u_i = e^{j\phi_i}$ as

$$\begin{aligned} &\max_{\boldsymbol{\theta}} \quad \min_{i} \left\{ \mathrm{Re}\left(\tfrac{1}{\sqrt{N_t}} \mathbf{h}_i e^{j(\boldsymbol{\theta} - \phi_i)} \right) \tan\omega - \left| \mathrm{Im}\left(\tfrac{1}{\sqrt{N_t}} \mathbf{h}_i e^{j(\boldsymbol{\theta} - \phi_i)} \right) \right| \right\} \\ &\text{subjectto } |\theta_n| \leq \pi, \forall n \in \{1, \ldots, N\}. \end{aligned} \tag{4.45}$$

In line with its conventional counterpart in [52], the formulation in (4.45) is clearly non-convex, but can be efficiently solved via the cross-entropy method. It is demonstrated in [46] that the constructive CEP approach, by harvesting useful signal power from constructive interference, provides significant performance benefits compared to conventional CEP approaches. For the example of a large scale system with $N_t = 64, K = 12$, power gains of more than 5 dB were demonstrated in [46].

4.3 Constructive Interference for Harvesting Both Radiated Power and Useful Signal Power

The recent research attention on energy harvesting from RF signals, the motivator behind this Book, has been stimulated from the fact that radiated energy can provide a useful source of wireless power. Complimentary to the discussion above where interfering energy is harvested as a source of useful signal power, recent works focus on the beamforming optimization where part of the signal is used for decoding and

part of it is harvested as wireless power, giving rise to the concept of simultaneous wireless information and power transfer (SWIPT) [55–57].

4.3.1 Constructive Interference in SWIPT

In the majority of SWIPT approaches, while interference is harvested as useful energy for powering the receiver's electronic components, in terms of signal detection interference is still treated as a harmful effect. In this section, we show that, by means of the constructive interference concept, interference can be harvested both as a source of wireless power *and* a source of useful signal power.

4.3.1.1 Conventional Beamforming for SWIPT

Beamforming approaches for SWIPT are based on the premise that part of the received signal is used for information decoding, while the rest of the signal power is used for energy harvesting at the receiver. When the receiver has only one antenna from which to both harvest energy and decode information, two practical receiver structures for SWIPT termed as "time switching" (TS) and "power splitting" (PS), are typically employed to separate the received signal for decoding information and harvesting energy [55]. For illustration reasons, at this point we focus on the PS approach, while the discussion in this section is trivially applicable to the TS approach.

A block diagram of the PS approach is shown in Fig. 4.12a, where it can be seen that a portion P_i of the received signal is used for decoding the signal, while the rest ($P_H = 1 - P_i$) is used for energy harvesting. In the figure, z_i models the noise from the signal conversion from RF to baseband.

Treating interference as harmful, the received SINR for user i is given by

$$\Gamma_i^{\text{con}} = \frac{|\mathbf{h}_i \mathbf{w}_i|^2}{\sum\limits_{k=1, k\neq i}^{K} |\mathbf{h}_i \mathbf{w}_k|^2 + N_0 + \frac{N_C}{P_i}}, \tag{4.46}$$

where N_C is the spectral density of the conversion noise z_i.

Similarly the harvested energy is typically expressed following the model in Fig. 4.12a as:

$$P_i^{\text{con}} = (1 - P_i) \left(\sum_{k=1}^{K} |\mathbf{h}_i \mathbf{w}_k|^2 + N_0 \right). \tag{4.47}$$

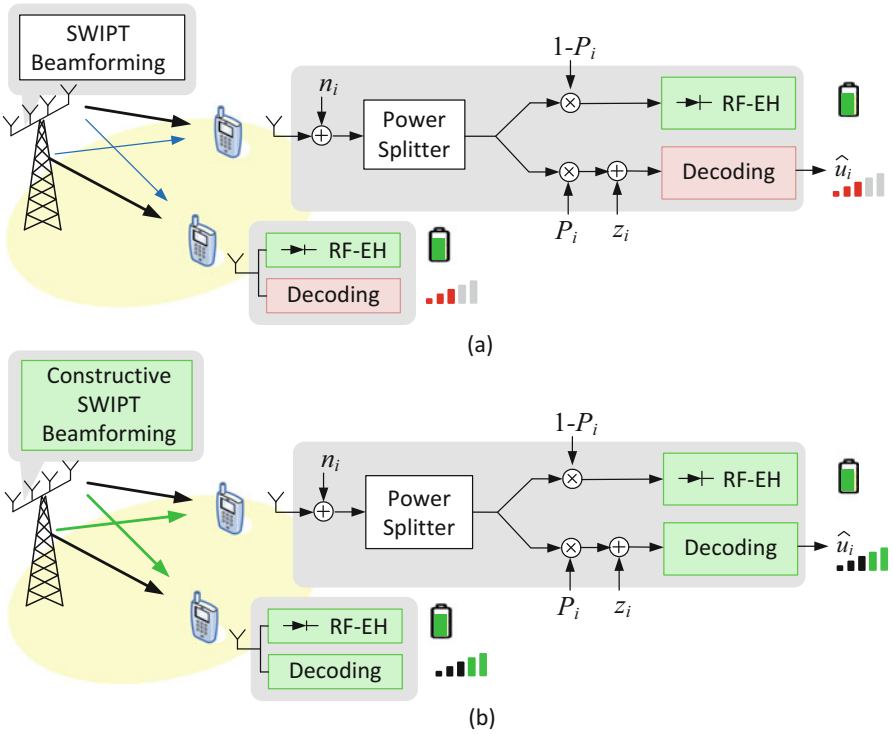

Fig. 4.12 Block diagram showing the power splitting SWIPT approach at the receiver with (**a**) SWIPT beamforming, (**b**) constructive SWIPT beamforming

Consequently, the power minimization problem with both QoS and EH constraints is formulated as

$$\begin{aligned} &\min_{\{\mathbf{w}_i, P_i\}} \sum_{i=1}^{K} \|\mathbf{w}_i\|^2 \\ &\text{s.t.} \quad \frac{|\mathbf{h}_i \mathbf{w}_i|^2}{\sum\limits_{k=1, k\neq i}^{K} |\mathbf{h}_i \mathbf{w}_k|^2 + N_0 + \frac{N_C}{P_i}} \geq \Gamma_i, \\ &\qquad (1 - P_i)\left(\sum_{k=1}^{K} |\mathbf{h}_i \mathbf{w}_k|^2 + N_0\right) \geq E_i, \; 0 < P_i < 1, \forall i. \end{aligned} \tag{4.48}$$

It is easy to see that formulation (4.48) is non-convex and hence challenging to solve. Semidefinite programming relaxation is usually employed to solve the optimization [58]. It is evident in the above optimization that, while interference is treated as useful for energy harvesting, is still treated as harmful for information

decoding, as it reduces the SINR at the receiver. This is demonstrated in Fig. 4.12a by the red shaded decoding part. Accordingly, the beamformer tries to constrain the interference in the decoding part of the received power, to secure a QoS level.

4.3.2 Interference-Exploitation Beamforming for SWIPT

Clearly, like in the beamforming optimizations of Sect. 4.2.2, there is scope to modify the optimization constraints such that constructive interference is harvested both as a source of RF energy and a source of useful signal energy. By adapting the beamforming optimizations in (4.32), (4.33) to the new transmission model as per Fig. 4.12 and including the EH constraint, it is straightforward to see that the interference-exploitation SWIPT beamforming optimization can be written as

$$\begin{aligned}
&\min_{\{\mathbf{w}_i\}} \left\| \sum_{k=1}^{K} \mathbf{w}_k e^{j(\phi_k-\phi_i)} \right\|^2 \\
&\text{s.t.} \left| \text{Im}\left(\mathbf{h}_i \sum_{k=1}^{K} \mathbf{w}_k e^{j(\phi_k-\phi_i)} \right) \right| \leq \left(\text{Re}\left(\mathbf{h}_i \sum_{k=1}^{K} \mathbf{w}_k e^{j(\phi_k-\phi_i)} \right) - \sqrt{\Gamma_i \left(N_0 + \frac{N_C}{P_i} \right)} \right) \tan\omega, \\
&\quad \left| \mathbf{h}_i \sum_{k=1}^{K} \mathbf{w}_k e^{j(\phi_k-\phi_i)} \right| \geq \sqrt{\frac{E_i}{1-P_i}}, 0 < P_i < 1, \forall i
\end{aligned} \tag{4.49}$$

The problem (4.49) is nontrivial to solve because of the non-convex constraint $\left|\mathbf{h}_i \sum_{k=1}^{K} \mathbf{w}_k e^{j(\phi_k-\phi_i)}\right| \geq \sqrt{\frac{E_i}{1-P_i}}$. A number of SOCP bounds have been derived in [59] to obtain the beamforming vectors $\mathbf{w}_k$.

It is clear here that interference now provides a source of both RF power for harvesting and useful signal power for decoding, as demonstrated in Fig. 4.12b. The above approach has been shown to offer power gains of more than 15 dB compared to conventional SWIPT beamforming in an $N_t = 4, K = 4$ MU-MISO system.

4.3.3 Open Problems and Research Directions

The above sections have overviewed work carried out in the area of interference exploitation, that has received recent attention in the context of harvesting interfering power for energy efficient wireless transmission. While a body of work has already focused on exploiting wireless interference in a number of scenarios and under various approaches, the topic is quite broad, with wide potential in revisiting

existing interference-cancellation approaches in interference-limited transmission scenarios. Accordingly, there are numerous open problems in the area.

Information Theory An important pillar of research that is widely open in the interference-exploitation research to date is that of communication-theoretic analysis and optimization. To this date, the fundamental extent of the potential benefits from constructive interference is unknown, as there is a lack of information-theoretic studies to provide performance benchmarks for the scenarios of interest. The main limitation here is the fact that, as interference exploitation is modulation dependent, Shannonian analysis and capacity calculations that assume Gaussian signals cannot be applied. Instead modulation-dependent analysis is required, building on the more complex finite-constellation approaches [60]. The development of such an analysis would, however, provide a benchmark against which to measure the performance of existing approaches, and more importantly, pave the way for optimizing practical approaches for interference exploitation towards achieving the theoretically optimal.

CSI Robustness and Asynchronous Interference It could be suggested that interference-exploitation approaches may be more sensitive to CSI errors and asynchronicity, since they heavily depend on the careful superposition of the interfering signals. While initial studies on CSI-robust techniques have disproved this [26, 37], the analytical study of the effects of CSI errors and asynchronicity, and the design of robust techniques specifically tailored for interference exploitation is still an open topic in the literature. Given that practical systems operate with various forms of CSI quantization and errors, and are subject to asynchronicity this provides a very pragmatic research direction.

Multi-Level Modulation Initial work on the application of the concept of constructive interference for multi-level modulation such as QAM and star-QAM has been ongoing [8–11], primarily designing the optimization constraints for beamforming to accommodate constructive interference. It is yet to be explored, however, how to adaptively adjust the decision boundaries in the multi-level constellations to further benefit from constructive interference, as discussed in Sect. 4.1.2. This entails both signal-processing algorithms and analytical work to study the extent of the required constellation expansion, and how to optimally benefit for such an approach.

Advanced Scenarios and Applications Finally, the application of the concept of this chapter to more advanced scenarios is still widely open. While initial work has been ongoing related to multi-cell transmission [13–16] and to energy harvesting communications [59] as detailed above, both these areas are open to contributions in their various scenarios and existing solutions. Other exciting applications as, for example, the exploitation of self-interference in full-duplex communications, the application of this concept to emerging wireless paradigms such as distributed antenna systems, Cloud–RAN transmissions, amongst many others, are still untouched territory that provide grounds for future research directions.

In the coming generations of wireless networks where power efficiency will play a dominant role, harvesting energy from interference, both as RF power and as useful signal power, is a critical enabling solution. The abovementioned concept of constructive interference and the identified open problems provide scope for fruitful research for the years to come.

Acknowledgements The author would like to thank the researchers in the Department of Electrical and Electronic Engineering in University College London, Pierluigi Amadori, Adrian Garcia Rodriguez, and Ka Lung Law for the helpful discussions and assistance in developing the content of this chapter.

The financial support from the Royal Academy of Engineering, UK is gratefully acknowledged.

References

1. M. Costa, Writing on dirty paper. IEEE Trans. Inf. Theory **IT-29**, 439–441 (1983)
2. G. Zheng, I. Krikidis, C. Masouros, S. Timotheou, D.A. Toumpakaris, Z. Ding, Rethinking the role of interference in wireless networks. IEEE Commun. Mag. **52**(11), 152–158 (2014)
3. C. Masouros, T. Ratnarajah, M. Sellathurai, C. Papadias, A. Shukla, Known interference in the cellular downlink: a performance limiting factor or a source of green signal power? IEEE Commun. Mag. **51**(10), 162–171 (2013)
4. D.N.C. Tse, P. Viswanath, *Fundamentals of Wireless Communications* (Cambridge University Press, Cambridge, 2005)
5. C. Masouros, E. Alsusa, Soft linear precoding for the downlink of DS/CDMA communication systems. IEEE Trans. Veh. Technol. **59**(1), 203–215 (2010)
6. C. Masouros, E. Alsusa, Dynamic linear precoding for the exploitation of known interference in mimo broadcast systems. IEEE Trans. Wirel. Commun. **8**(3), 1396–1404 (2009)
7. 3GPP TS 36.211, V8.2.0 (2008-03), Release 8 Evolved Universal Terrestrial Radio Access (E-UTRA); Physical Channels and Modulation
8. F. Keskin, J. Hahn, P.W. Baier, Minimum energy soft precoding. Electron. Lett. **43**(6), 55–56 (2007)
9. M. Li, C. Liu, S.V. Hanly, Transmitter optimization for the network mimo downlink with finite-alphabet and QoS constraints, in *AusCTW* Adelaide, 2013
10. M. Alodeh, S. Chatzinotas, B. Ottersten, Constructive interference through symbol level precoding for multi-level modulation, in *2015 IEEE Global Communications Conference (GLOBECOM)*, San Diego, CA, 2015
11. M. Alodeh, S. Chatzinotas, B. Ottersten, Symbol-level multiuser MISO precoding for multi-level adaptive modulation: a multicast view (2016). arXiv preprint arXiv:1601.02788
12. D. Kwon, W. Yeo, D.K. Kim, A new precoding scheme for constructive superposition of interfering signals in multiuser MIMO systems. IEEE Commun. Lett. **18**(11), 2047–2050 (2014)
13. F. Khan, C. Masouros, T. Ratnarajah, Interference driven linear precoding in multiuser MISO downlink cognitive radio network. IEEE Trans. Veh. Technol. **61**(6), 2531–2543 (2012).
14. C. Masouros, T. Ratnarajah, Interference as a source of green signal power in cognitive relay assisted co-existing MIMO wireless transmissions. IEEE Trans. Commun. **60**(2), 525–536 (2012)
15. K.L. Law, C. Masouros, M. Pesavento, Transmit beamforming for interference exploitation in the underlay cognitive radio Z-channel. IEEE Trans. Signal Process. (submitted). Available on https://arxiv.org/abs/1606.06504

16. M. Alodeh, S. Chatzinotas, B. Ottersten, Symbol based precoding in the downlink of cognitive MISO channel, in *Proceedings of CROWNCOM* (2015)
17. C. Masouros, E. Alsusa, Two-stage transmitter precoding based on data-driven code hopping and partial zero forcing beamforming for MC-CDMA communications. IEEE Trans. Wirel. Commun. **8**(7), 3634–3645 (2009)
18. C. Masouros, E. Alsusa, Interference exploitation using adaptive code allocation for the downlink of precoded MC-CDMA systems. IET J. Commun. **2**(9), 1118–1130 (2008). doi:10.1049/iet-com:20070628
19. E. Alsusa, C. Masouros, Adaptive code allocation for interference management on the downlink of DS-CDMA systems. IEEE Trans. Wirel. Commun. **7**(7), 2420–2424 (2008). doi:10.1109/TWC.2008.061043
20. C. Masouros, Correlation rotation linear precoding for MIMO broadcast communications. IEEE Trans. Signal. Process. **59**(1), 252–262 (2011)
21. S.M. Razavi, T. Ratnarajah, C. Masouros, Transmit-power efficient linear precoding utilizing known interference for the multiantenna downlink. IEEE Trans. Veh. Technol. **63**(9), 4383–4394 (2014)
22. S.M. Razavi, T. Ratnarajah, Adaptively regularized phase alignment precoding for multiuser multiantenna downlink. IEEE Trans. Veh. Technol. **64**(10), 4863–4869 (2015)
23. M.-J. Qi, Y.-C. Wu, Correlation rotation precoding algorithm based on criterion of minimum mean square error. J. Comput. Appl. **1**, 037 (2012)
24. X.M. Yang, Y. Xiong, Linear precoding with known interference for MIMO broadcast channels. Electron. Lett. **47**(13), 778–780 (2011)
25. Z.J. Liu, J.L. Wang, D.C. Sun K.C. Yi, Unified SER performance analysis and improvement for multiuser MIMO downlink with correlation rotation linear precoding. IEEE Trans. Wirel. Commun **12**(4), 1678–1685 (2013)
26. D. Kwon, H.S. Kang, D.K. Kim, Robust interference exploitation-based precoding scheme with quantized CSIT. IEEE Commun. Lett. **20**(4), 780–783 (2016)
27. C.B. Peel, B.M. Hochwald, A.L. Swindlehurst, A vector-perturbation technique for near-capacity multiantenna multiuser communication-part I: channel inversion and regularization. IEEE Trans. Commun. **53**(1), 195–202 (2005)
28. C. Windpassinger, R. Fischer, T. Vencel, J. Huber, Precoding in multiantenna and multiuser communications, IEEE Trans. on Wireless Comms. **3**(4), 1305–1316 (2004)
29. C.B. Peel, B.M. Hochwald, A.L. Swindlehurst, A vector-perturbation technique for near-capacity multiantenna multiuser communication-part II: perturbation. IEEE Trans. Commun. **53**(3), 537–544 (2005)
30. C. Masouros, M. Sellathurai, T. Ratnarajah, Interference optimization for transmit power reduction in Tomlinson-Harashima precoded MIMO downlinks. IEEE Trans. Signal Process. **60**(5), 2470–2481 (2012)
31. A. Garcia, C. Masouros, Power-efficient Tomlinson-Harashima precoding for the downlink of multi-user MISO systems. IEEE Trans. Commun. **62**(6), 1884–1896 (2014)
32. E. Agrell, T. Eriksson, A. Vardy, K. Zeger, Closest point search in lattices. IEEE Trans. Inf. Theory **48**(8), 2201–2214 (2002)
33. C. Masouros, M. Sellathurai, T. Ratnarajah, Vector perturbation based on symbol scaling for limited feedback MISO downlinks. IEEE Trans. Signal Process. **62**(3), 562–571 (2014)
34. M. Bengtsson, B. Ottersten, Optimal and suboptimal transmit beamforming, in *Handbook of Antennas in Wireless Communications*, ed. by L. Godara, ch. 18 (CRC, Boca Raton, FL, 2001)
35. M. Schubert, H. Boche, Solution of the multi-user downlink beamforming problem with individual SINR constraints. IEEE Trans. Veh. Technol. **53**(1), 18–28 (2004)
36. M. Alodeh, S. Chatzinotas, B. Ottersten, Constructive multiuser interference in symbol level precoding for the MISO downlink channel. IEEE Trans. Signal Process. **63**(9), 2239–2252 (2015)

37. C. Masouros, G. Zheng, Exploiting known interference as green signal power for downlink beamforming optimization. IEEE Trans. Signal Process. **63**(14), 3668–3680 (2015)
38. M. Alodeh, S. Chatzinotas, B. Ottersten, Energy-efficient symbol-level precoding in multiuser MISO based on relaxed detection region. IEEE Trans. Wirel. Commun. **15**(5), 3755–3767 (2016)
39. K.L. Law, C. Masouros, K.K. Wong, G. Zheng, Constructive interference exploitation for QoS-based downlink beamforming optimization. IEEE Trans. Signal Process. (in press)
40. A. Li, C. Masouros, Exploiting constructive mutual coupling in P2P MIMO by analog-digital phase alignment. IEEE Trans. Wirel. Commun. **16**(3), 1948–1962 (2017)
41. C. Masouros, E. Alsusa, Transmit antenna selection for partial linear precoding MIMO schemes. IET Electron. Lett. **45**(14), 736–737 (2009)
42. P.V. Amadori and C. Masouros, interference driven antenna selection for massive multi-user MIMO. IEEE Trans. Veh. Technol. **65**(8), 5944–5958 (2016)
43. P.V. Amadori, C. Masouros, Large scale antenna selection for interference exploitation. IEEE Trans. Commun. (in press)
44. M. Alodeh, S. Chatzinotas, B. Ottersten, Data aware user selection in the cognitive downlink MISO precoding systems, in *IEEE International Symposium on Signal Processing and Information Technology (ISSPIT)*, December 2013. Invited paper
45. Z. Ding, Z. Yang, P. Fan, H.V. Poor, On the performance of non-orthogonal multiple access in 5G systems with randomly deployed users. IEEE Signal Process. Lett. **21**(12), 1501–1505 (2014)
46. P.V. Amadori, C. Masouros, Constant envelope precoding by interference exploitation in phase shift keying-modulated multiuser transmission. IEEE Trans Wirel. Commun. **16**(1), 538–550 (2017)
47. X. Gao, O. Edfors, F. Tufvesson, E.G. Larsson, Massive MIMO in real propagation environments: do all antennas contribute equally? IEEE Trans. Commun. **63**(11), 3917–3928 (2015)
48. Z. Chen, J. Yuan, B. Vucetic, Z. Zhou, Performance of Alamouti scheme with transmit antenna selection, in *IEEE International Symposium on Personal, Indoor and Mobile Radio Communications*, vol. 2 (2004), pp. 1135–1141
49. F. Rusek, D. Persson, B.K. Lau, E. Larsson, T. Marzetta, O. Edfors, F. Tufvesson, Scaling up MIMO: opportunities and challenges with very large arrays. IEEE Signal Process. Mag. **30**(1), 40–60 (2013)
50. A. Gorokhov, D. Gore, A. Paulraj, Receive antenna selection for MIMO spatial multiplexing: theory and algorithms. IEEE Trans. Signal Process. **51**(11), 2796–2807 (2003)
51. Y. Cheng, M. Pesavento, Joint discrete rate adaptation and downlink beamforming using mixed integer conic programming. IEEE Trans. Signal Process. **63**(7), 1750–1764 (2015)
52. S.K. Mohammed, E.G. Larsson, Per-antenna constant envelope precoding for large multi-user MIMO systems. IEEE Trans. Commun. **61**(3), 1059–1071 (2013)
53. J.C. Chen, C.K. Wen, K.K. Wong, Improved constant envelope multiuser precoding for massive MIMO systems. IEEE Commun. Lett. **18**(8), 1311–1314 (2014)
54. P.T. De Boer, D.P. Kroese, S. Mannor, R.Y. Rubinstein, A tutorial on the cross-entropy method. Ann. Oper. Res. **134**(1), 19–67 (2005)
55. R. Zhang, C.K. Ho, MIMO broadcasting for simultaneous wireless information and power transfer. IEEE Trans. Wirel. Commun. **12**(5), 1989–2001 (2013)
56. G. Zhu, C. Zhong, H.A. Suraweera, G.K. Karagiannidis, Z. Zhang, T.A. Tsiftsis, Wireless information and power transfer in relay systems with multiple antennas and interference. IEEE Trans. Commun. **63**, 1400–1418 (2015)
57. Y. Zeng, R. Zhang, Full-duplex wireless-powered relay with self-energy recycling. IEEE Wirel. Commun. Lett. **4**(2), 201–204 (2015)

58. S. Timotheou, I. Krikidis, G. Zheng, B. Ottersten, Beamforming for MISO interference channels with QoS and RF energy transfer. IEEE Trans. Wirel. Commun. **13**(5), 2646–2658 (2014)
59. S. Timotheou, G. Zheng, C. Masouros, I. Krikidis, Exploiting constructive interference for simultaneous wireless information and power transfer in multiuser downlink systems. IEEE JSAC Spec. Issue Green Commun. Netw. Second Issue **34**(5), 1772–1784 (2016)
60. W. He, C.N. Georghiades, Computing the capacity of a MIMO fading channel under PSK signaling. IEEE Trans. Inform. Theory **51**(5), 1794–1803 (2005)